Appendix O

→ JMT

Are Single Molecular Wires Conducting?

L. A. Bumm, J. J. Arnold, M. T. Cygan, T. D. Dunbar, T. P. Burgin, L. Jones II, D. L. Allara,* J. M. Tour,* P. S. Weiss*

Molecular wire candidates inserted into "nonconducting" *n*-dodecan · thiol self-assembled monolayers on Au{111} have been probed by scanning tunneling microscopy (STM) and microwave frequency alternating current STM (ACSTM) at high tunnel junction impedance (100 GΩ) to assess their electrical properties. The inserted conjugated molecules, 4,4′-di(phenylene-ethynylene)benzenethiolate derivatives, form single molecular wires (MWs) which extend from the Au{111} substrate to *ca.* 7Å above and have very high conductivity compared t the alkanethiolate.

L. A. Bumm, J. J. Arnold, M. T. Cygan, T. D. Dunbar, P. S. Weiss, Department of Chemistry, The Pennsylvania State University, University Park, PA 16802, USA.

D. L. Allara, Departments of Chemistry and Materials Science, The Pennsylvania State University, University Park, PA 16802, USA.

T. P. Burgin, L. Jones II, J. M. Tour, Department of Chemistry and Biochemistry, University of South Carolina, Columbia, SC 29208, USA.

---

*To whom correspondence should be addressed.

To appear in
~~Revised for~~
Science

→ JMT

Are Single Molecular Wires Conducting?

L. A. Bumm, J. J. Arnold, M. T. Cygan, T. D. Dunbar, T. P. Burgin, L. Jones II, D. L. Allara,* J. M. Tour,* P. S. Weiss*

Molecular wire candidates inserted into "nonconducting" *n*-dodecan - thiol self-assembled monolayers on Au{111} have been probed by scanning tunneling microscopy (STM) and microwave frequency alternating current STM (ACSTM) at high tunnel junction impedance (100 GΩ) to assess their electrical properties. The inserted conjugated molecules, 4,4′-di(phenylene-ethynylene)benzenethiolate derivatives, form single molecular wires (MWs) which extend from the Au{111} substrate to ca. 7Å above and have very high conductivity compared t the alkanethiolate.

L. A. Bumm, J. J. Arnold, M. T. Cygan, T. D. Dunbar, P. S. Weiss, Department of Chemistry, The Pennsylvania State University, University Park, PA 16802, USA.

D. L. Allara, Departments of Chemistry and Materials Science, The Pennsylvania State University, University Park, PA 16802, USA.

T. P. Burgin, L. Jones II, J. M. Tour, Department of Chemistry and Biochemistry, University of South Carolina, Columbia, SC 29208, USA.

---

*To whom correspondence should be addressed.

To appear in
~~Revised for~~
Science

Molecular wires (MWs) are among the key components in the emerging field of molecular electronics. In their simplest form, MWs can be viewed as conjugated molecules which form the one–dimensional electronic conductors to interconnect such proposed molecular devices as single electron transistors (SET), electron turnstiles, molecular switches, and chemical sensors *(1)*. Although many MW candidates have been prepared *(2)*, the conductivity of *single* MWs has not been demonstrated. This is due in part to the difficulty of individually connecting a *single* MW to probes which in turn are connected to macroscopic measuring instruments in the laboratory. In this report we describe how molecular self–assembly has been used both to anchor a MW candidate to an electrode (the Au{111} substrate) and to dilute and isolate the MW candidates within a self–assembled monolayer (SAM) of *n*–dodecanethiol (DT). The second connection to the MW candidate is achieved via the probe tip of a scanning tunneling microscope (STM) or a tunable microwave frequency alternating current STM (ACSTM). The individual molecules can be observed in conventional STM images as well as by their microwave frequency electronic properties. The STM can then individually address the inserted MW candidates and probe their electronic properties.

Bulk conductivity measurements of MW candidates include both conduction paths along the molecule and (percolation) between the chains. Wu & Bein have grown isolated polyaniline molecules *(3)* and graphitic carbon *(4)* in zeolite matrices to eliminate inter–chain percolation and have demonstrated the molecules' conductivity using a microwave cavity perturbation technique at 2.63 GHz. Jones *et al. (5)* have made preliminary measurements using mechanical break junctions (MBJs) containing 1,4–benzenedithiol. Unfortunately, these tunnel junctions are ill–defined in that it is difficult to know if the conducting channel is a single molecule, or even the molecule of interest. The STM and ACSTM are ideal for this study because they allow us to image the surface and locate isolated molecules. These molecules are then individually addressed.

The MW candidate used was an ethyl substituted 4,4′–di(phenylene–ethynylene)–benzothioacetate (**1**) has been shown to self–assemble on Au when converted to the thiolate (**1′** in Fig. 1) *(6)*. The calculated length of **1′**, 21.3 Å *(7)*, is 7.3 Å longer than the thickness of the DT monolayer on Au{111} *(8)* so that when coadsorbed it is expected to protrude beyond the

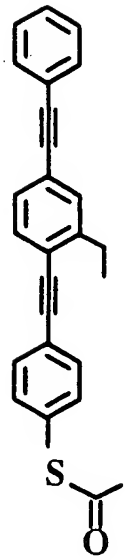

1

methyl–terminated surface (Fig. 1). Even if tilted at the 30° angle of the DT molecules, the **1′** molecules would still protrude 4.0Å above the DT film. Molecular modeling indicates that the **1′** molecules do not fit well into the DT lattice because of spatial constraints and poor van der Waals overlap with the surrounding DT molecules.

The SAM was prepared on Au{111}, which had been vapor deposited onto freshly–cleaved, heated muscovite mica. The Au substrate was exposed to a 1 mM solution of DT in ethanol for 18 hr. to form a well–ordered monolayer *(9)*. After thoroughly rinsing the sample *(10)*, it was exposed to a 0.3 mM solution of **1** in tetrahydrofuran under dry Ar for 30 min. A small amount of aqueous ammonia was added to hydrolyze the thioacetyl protecting group, generating the thiol *in situ* to adsorb as the thiolate (**1′**) on the surface *(6)* as shown schematically below. Note that we do not expect voids at the structural domain boundaries (as shown in the schematic), but rather conformationally relaxed DT molecules filling these spaces (*11*). After rinsing and drying *(10)*, the samples were stored at room temperature until imaged; exposure to air was limited. These SAMs were characterized by ellipsometry and by reflectance infrared spectroscopy *(12)*.

Previously, we have shown STM images of phase segregated ω–substituted alkanethiolate monolayers on Au{111} *(9)*. Furthermore we can differentiate between *n*–alkanethiolates of different chain lengths with molecular resolution in mixed composition SAMs *(13)*. In this report, we use the DT monolayer as a matrix to support and to dilute the candidate MWs. Tour *et al.* have

shown that **1′** chemisorbs to Au{111} forming close-packed SAMs with the long molecular axis aligned nearly normal to the surface *(6)*. Cygan *et al.* have demonstrated that the **1′** adsorbs into an existing DT SAM at film defects, *e.g.* domain boundaries *(12)*, where the DT molecules can be conformationally relaxed. In contrast to neat **1′** SAMs where the molecules can be oriented normal to the Au{111}, the molecular orientation might vary due to being imbedded in the DT film and further due to conformational relaxation of the surrounding DT molecules at structural domain boundaries.

The STM and microwave frequency ACSTM used in these experiments have been described elsewhere *(14)*. We measure the high frequency conductivity of the tunnel junction by adding microwave frequency components to the conventional DC bias. In order to simplify detection of the high frequency tunnel current we simultaneously apply two frequencies separated by 5 kHz. The component of the tunnel current at the difference frequency is then extracted with a phase-sensitive detector. That this nonlinear scheme truly measures a high frequency property of the tunnel junction can be understood as an application of Miller's rule *(15)*. Namely, the n^{th}-order susceptibility for difference frequency generation is proportional to the product of the first-order susceptibilities at the frequency of each input and output *(16)*.

STM images of the DT and **1′** SAM are shown in Figs. 2A and 2B. We assign the (bright) topographic features protruding through the DT film as due to **1′** since these features are not observed in the DT films prior to exposure to the solution of **1**. We infer that these features are due to single **1′** molecules from the following observations: 1) images of these features where the DT molecular lattice is resolved show that the single-**1′** molecular features are imaged with exactly the same shape, size, and orientation, indicative of features which are much sharper than the STM tip (Fig. 2B); 2) larger features (which we assign to clusters of **1′**) are only observed at Au{111} step edges where the DT SAM is expected to be conformationally relaxed and the **1′** molecules would be more easily accommodated (Fig. 2A); 3) the **1′** molecules are observed to be widely separated on the terraces (Fig. 2A) and tend to occur at DT structural domain boundaries (Figs. 2A and 2B) — only a small fraction of the DT structural domain boundaries on the Au{111} terraces are occupied by **1′** features indicating that their insertion into the film is an isolated and improbable event; and 4)

direct insertion of clusters is unlikely because **1** is not known to be associated (dimers, etc.) in solution phase. The DT film forms domains of $(\sqrt{3}\times\sqrt{3})$ R30° and related superstructures *(17)*. Structural domain boundaries result from different alkyl chain tilt vectors and sulfur–head–group–lattice registry. The dark features are due to the underlying Au substrate which frequently develops single atomic layer deep pits during exposure to alkanethiol solution *(18)*. The **1′** molecules have been observed for as long as 4 hrs and did not move or wander though the DT film. At the same time the boundaries between the structural domains fluctuate as molecules at these interfaces change their conformations.

STM topographic images are a convolution of the tip and surface geometry. When features on the surface are much sharper than the tip, such as the **1′** single molecular protrusion *ca.* 7 Å higher than the DT film, each molecule is rendered as an image of the tip. This is shown schematically in Fig. 1 and can be seen in the images of **1′** molecules (Fig. 2B) where each appears nearly identical in shape, size, and orientation. If more than a single **1′** molecule were adjacent at the structural domain boundaries, each would contribute to the tunneling current. Thus the "tip image" from such a feature would be repeated and overlapped in a characteristic way. This is rarely found at the structural domain boundaries on terraces, but is commonly found for the **1′** molecules at substrate step edges. It is instructive to note that most molecular resolution images are achieved on atomically flat surfaces so that sharpness of the tip is determined only by the endmost atomic–scale asperity. Here, with the same tip, we do resolve the molecular lattice on the flat DT regions.

The apparent tunneling barrier height (ATBH) can be measured using the STM by modulating the separation between the tip and sample (z) and recording the derivative of the tunneling current (I) with respect to this separation (dI/dz) *(20)*. The ATBH is at least 2 times higher over the **1′** than over the DT. This higher relative ATBH, concurrent with greater tip–substrate separation (as shown schematically in Fig. 1), indicates that the junction contains regions of higher conductivity when the tip is over a **1′** molecule than when over a DT molecule. Hence we infer that single **1′** molecules have a higher conductivity than the DT. We will not attempt to quantify the ATBH further because many factors come into play such as mechanical distortions of the tip and film. These complications make more than qualitative comparisons difficult at best *(19,20)*.

Figure 3 shows both the constant current STM topography (shown as surface topography) and the simultaneously acquired microwave difference frequency (MDF) ACSTM image (shown as surface color). Four types of features can be seen: 1) topographic maxima which coincide with MDF maxima; 2) a single topographic maximum that does not coincide with the MDF maxima; 3) MDF maxima that coincide with protrusions at DT film defects; and 4) a Au{111} substrate atomic step is also visible.

The mechanism by which insulating molecules, such as DT monolayers, are imaged with the STM remains poorly understood *(19)*. In contrast, the MW does have states which are accessible by STM. This is evident in the DC STM, apparent tunneling barrier height, and ACSTM microwave difference frequency images.

The interpretation of STM topographic height differences is complicated because they are a function of the local density of states as well as the local barrier height *(21)*. However, four observations lead us to infer that the **1′** molecules are substantially more conducting than DT: 1) unlike *n*–alkanethiols of similar length, *viz.* 20 carbon *n*–alkanethiols *(eicosanethiol)*, the **1′** molecules can be imaged nonperturbatively *(22)*; 2) the apparent tunneling barrier height is higher over the **1′** molecules despite their greater topographic height; 3) we observe distinct contrast in the MDF images between the DT and the **1′** molecules which is not observed for neat DT films or for SAMs of *n*–alkanethiols of mixed chain length; and 4) the differences in the topographic height in DC STM images between the DT and **1′** molecules increase with decreasing junction impedance. Currently, we are spectroscopically mapping **1′** and other related molecules inserted into alkanethiol SAMs to further delineate single molecular wire performance.

REFERENCES AND NOTES

1. A. Aviram, Ed., *Molecular Electronics: Science and Technology*, Confer. Proc. No. 262, American Institute of Physics: New York, 1992; M. A. Reed and W. P. Kirk, Eds., *Nanostructure Physics and Fabrication* (Academic Press, Inc., New York, NY, 1989); M. A. Reed and W. P. Kirk, Eds., *Nanostructures and Mesoscopic Systems* (Academic Press, Inc., New York, NY, 1992); F. L. Carter, Ed., *Molecular Electronic Devices II* (Marcel Dekker, Inc., New York, NY, 1987); J. S. Miller, *Adv. Mater.* **2**, 378, 495, 601 (1990).
2. J. M. Tour, *Trends in Polym. Sci.* **2**, 332 (1994).
3. C.–G. Wu and T. Bein, *Science* **264**, 1757 (1994).
4. C.–G. Wu and T. Bein, *Science* **266**, 1013 (1994).
5. L. Jones II *et al.*, *Polym. Prepr.* **36,** 564 (1995).
6. J. M. Tour *et al.*, *J. Am. Chem. Soc.* **117**, 9529 (1995).
7. J. S. Schumm, D. L. Pearson, J. M. Tour, *Angew. Chem. Int. Ed. Engl.* **33**, 1360 (1994).
8. L. H. Dubois and R. G. Nuzzo, *Annu. Rev. Phys. Chem.* **43**, 437 (1992), and references therein.
9. S. J. Stranick, A. N. Parikh, Y.–T. Tao, D. L. Allara, P. S. Weiss, *J. Phys. Chem.* **98**, 7636 (1994).
10. The substrates treated with DT in ethanol were rinsed sequentially in hexane, acetone, and ethanol and then blown dry in purified N_2. The substrates further treated with **1** in tetrahydrofuran were rinsed sequentially in tetrahydrofuran, acetone, and ethanol and then blown dry in purified N_2. See ref. 12 for the complete procedure.
11. S. J. Stranick, A. N. Parikh, D. L. Allara, P. S. Weiss, *J. Phys. Chem.* **98**, 11136 (1994).
12. M. T. Cygan *et al.*, in preparation.
13. L. A. Bumm *et al.*, in preparation.
14. S. J. Stranick and P. S. Weiss, *Rev. Sci. Instrum.* **64**, 1232 (1993); S. J. Stranick and P. S. Weiss, *ibid.* **65**, 918 (1994); L. A. Bumm and P. S. Weiss, *ibid.* **66**, 4140 (1995).
15. R. C. Miller, *Appl. Phys. Lett.* **5**, 17 (1964).

16. The exact mechanism of the microwave difference frequency contrast is not yet established. Possible mechanisms include heating (square law), difference frequency generation (ω_{out}: ω_1; ω_2); modulated conductivity (ω_{out}: 0: ω_1; ω_2). Each of these mechanisms are linearly dependent on the power at *each* input frequency. Thus, we can measure the response of the tunnel junction at GHz frequencies by detecting a signal at 5 kHz.

17. G. E. Poirier and M. J. Tarlov, *Langmuir* **10**, 2853 (1994); G. E. Poirier, M. J. Tarlov, H. E. Rushmeier, *ibid.* **10**, 3383 (1994).

18. J. A. M. Sondag–Huethorst, C. Schönenberger, L. G. J. Fokkink, *J. Phys. Chem.* **98**, 6827 (1994).

19. V. Mujica, M. Kemp, M. A. Ratner, *J. Chem. Phys.* **101**, 6856 (1994).

20. See, for example, C. J. Chen, *Introduction to Scanning Tunneling Microscopy* (Oxford University Press, New York, NY 1993).

21. N. D. Lang, *Phys. Rev. Lett.* **58**, 45 (1987); N. D. Lang, *Phys. Rev. B* **37**, 10395 (1988).

22. C. Schönenberger, J. Jorritsma, J. A. M. Sondag–Huethorst, L. G. J. Fokkink, *J. Phys. Chem.* **99**, 3259 (1995).

23. We thank Wolfgang Ernst for the loan of a microwave source. The support of ARPA, the NSF Chemistry, GRT, Materials Research, and PYI Programs, the ONR, AT&T Bell Laboratories, the Biotechnology Research and Development Corporation, Eastman Kodak, Hewlett–Packard, IBM, and the Alfred P. Sloan Foundation are gratefully acknowledged.

FIGURE CAPTIONS

Fig. 1. A schematic representation of a DT and **1'** SAM on Au{111}. The height that **1'** extends above the DT film, if normal to the surface, is 7.3 Å. The trajectory of the STM tip traces out a surface of constant current. The relatively flat DT layer can be imaged by an atomic–scale asperity on the end of the STM tip with resolution of the molecular lattice. The protruding **1'** molecule "images" the end of the STM tip, resulting in a characteristic feature due largely to the shape of the end of the STM tip for each **1'** molecule, as seen in subsequent figures. Note also that the STM tip is closer to the exposed ends of the **1'** molecules than to the exposed ends of the DT molecules. This is because the apparent tunneling barrier height is higher over the **1'** than over the DT.

Fig. 2. Constant current STM topographs of an Au{111} surface covered by DT and **1'** (tip bias +1.0 V, tunneling current 10 pA). A) A 2400Å by 2400Å image which has been displayed (by high–pass filtering) to show the distribution of **1'** molecules on several terraces simultaneously. Note that the **1'** molecules on the Au terraces are widely separated and of uniform size as opposed to the larger features at the Au step edges which we assign as clusters of **1'** molecules. B) An unprocessed 400Å by 400Å image showing DT molecular lattice resolution. Note the two **1'** molecules adsorbed at DT structural domain boundaries in the lower right quadrant of the image. The apparent shape of **1'** is a characteristic of this tip, rather than of the molecule itself. These two **1'** molecules were observed to be stationary in the DT film for over 4 hrs.

Fig. 3. A composite ACSTM image showing a 800Å by 800Å area of a Au{111} surface covered by DT and **1'**. The surface is derived from the constant current topograph and the color from the MDF signal (DC tip bias +1.0 V, DC tunneling current 10 pA,

microwave frequencies 5.00000000 GHz and 5.00000500 GHz applied to the ACSTM tip transmission line at *ca.* 1mW each, detection at 5 kHz).

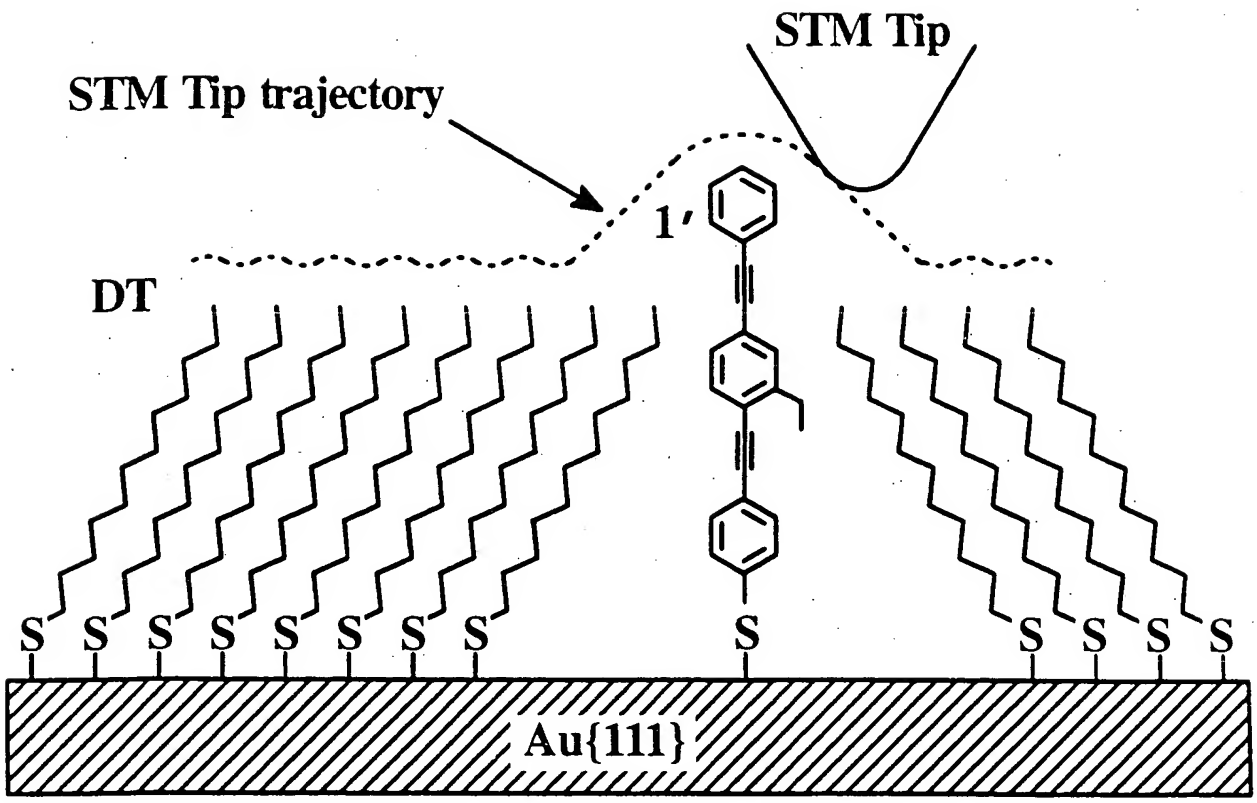

Fig. 1

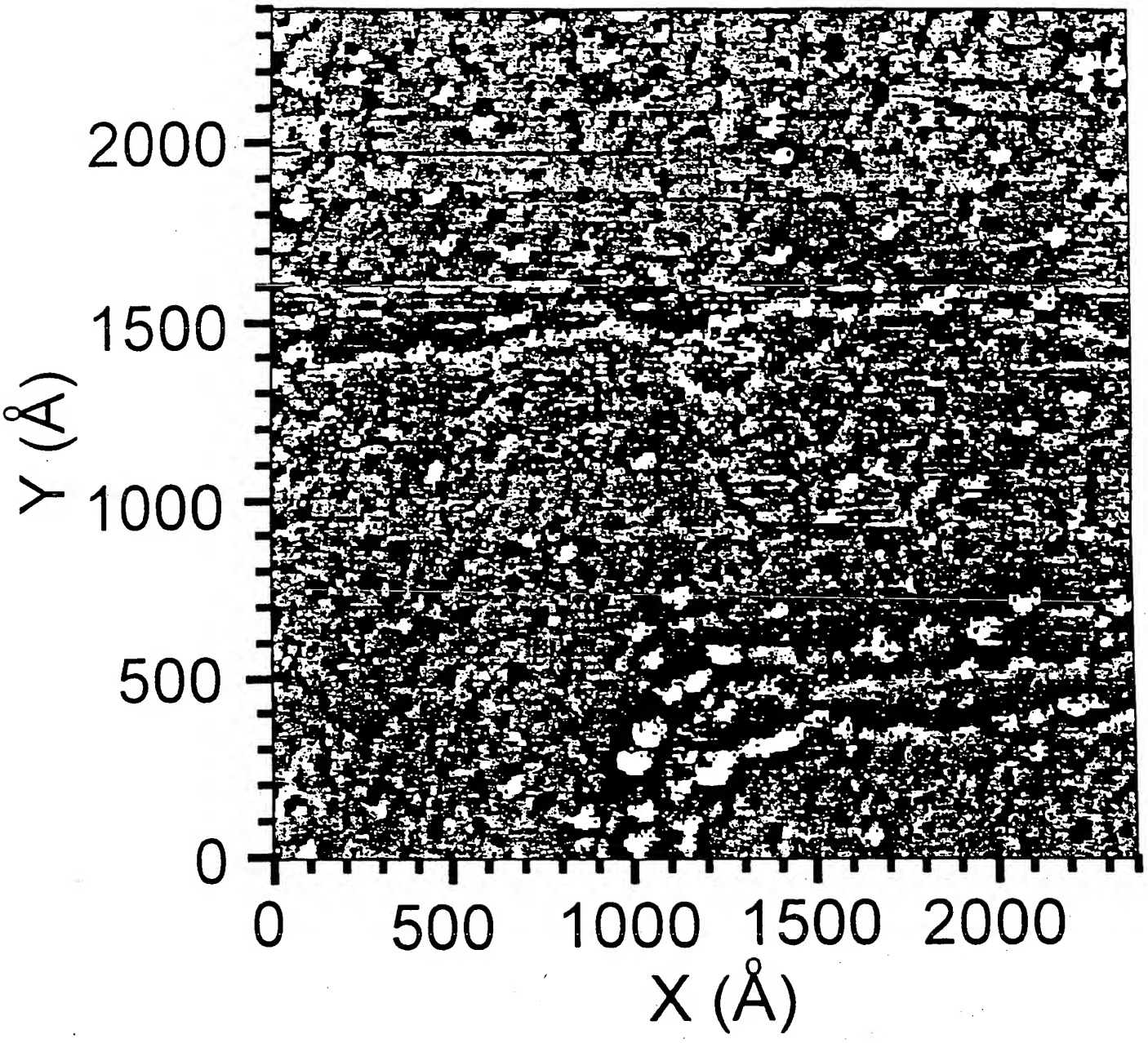

Fig 2a

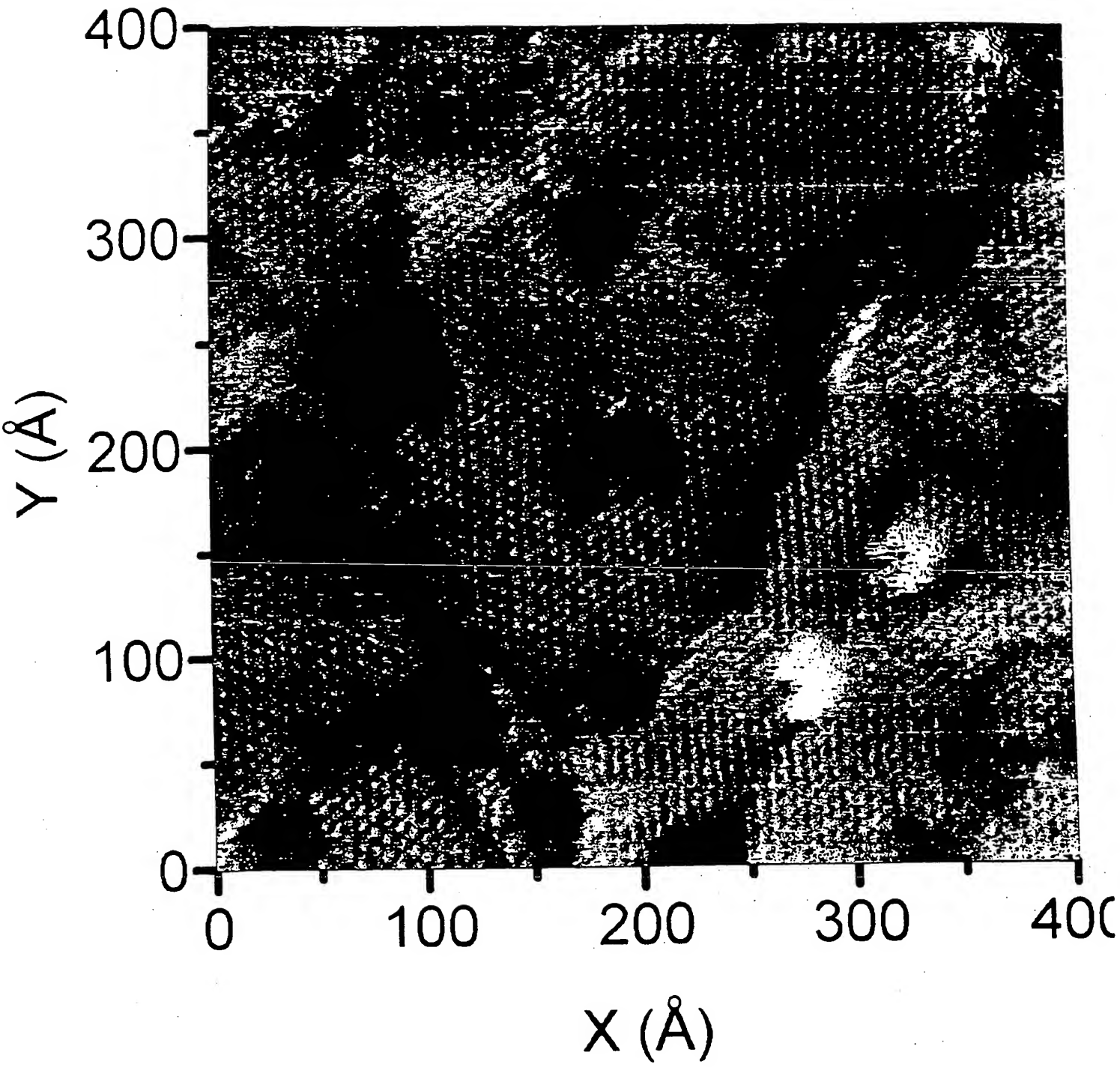

Fig 2b

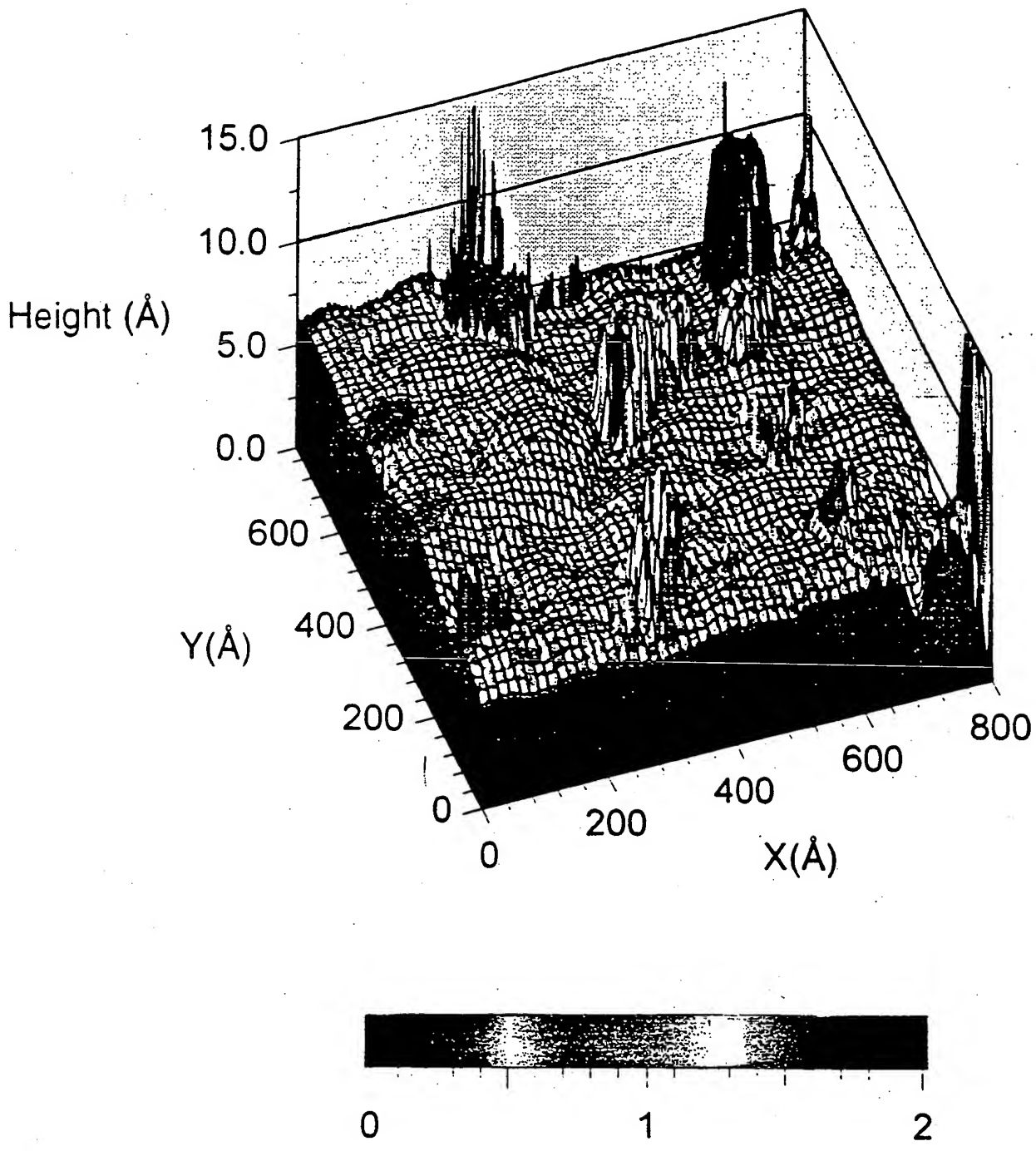
15.0
10.0
Height (Å)
5.0
0.0
600
400
Y(Å)
200
0
0
200
400
600
800
X(Å)
0
1
2
Current at 5 KHz Difference Frequency (pA rms)

Fig 3